JOURNAL OF MATERIALS SCIENCE **40** (2005) 3911 – 3915

Influence of milling media on the microstructure and mechanical properties of mechanically milled and sintered aluminium

J. CINTAS*, J. M. MONTES, F. G. CUEVAS, E. J. HERRERA
Grupo de Metalurgia e Ingeniería de los Materiales, ETS de Ingenieros, Universidad de Sevilla, Camino de los Descubrimientos s/n, 41092 Sevilla, Spain
E-mail: jcintas@esi.us.es

Mechanically alloyed aluminium powder was prepared by vacuum attrition milling. Two types of milling balls (steel or hard-metal balls) were employed. Powder consolidation was carried out by cold pressing and vacuum sintering. The microstructure of consolidated samples obtained from powder milled with steel balls shows needle-shaped Al-Fe intermetallics. This acicular morphology is responsible for the low elongation (1%) of these samples. However, specimens manufactured from powder milled with hard-metal balls show a different microstructure. The powder is contaminated by WC and Co, coming from the milling balls. These contaminants change the size (smaller) and the shape (spheroidal) of the intermetallics. This results in a remarkable increase in elongation (4%), without reduction in tensile strength (ca. 300 MPa).

1. Introduction

In recent years, mechanical alloying/milling has acquired a widespread recognition as a technique whereby chemical reactions and alloying are induced in a variety of powder systems [1, 2]. Supersaturated solid solutions, even of immiscible species, non-equilibrium phases, amorphous materials, and nanostructured powders can be successfully obtained by high-energy milling processing [3–5].

In particular, mechanically alloyed aluminium, MA Al, powder can be prepared by attrition milling of Al powder [6]. During milling, Al particles undergo severe plastic deformation and are brought into intimate contact forming cold welds. With continued plastic deformation, the hardness of the powder increases and repetitive fracture occurs. A process control agent, PCA, usually a wax powder, is added to prevent excessive welding of aluminium to itself, balls, impeller and attritor vessel, and to establish a dynamic balance between fracturing and welding.

An additional task of the PCA is to react with aluminium to form carbides. MA Al particles are actually nanograined composite particles [7], that contain a fine and homogeneous distribution of submicroscopic ceramic (Al_2O_3, Al_4C_3) dispersoids [8]. So, MA Al powder is very hard and, therefore, its compressibility is low.

The properties of MA Al powders are very sensitive [6] to experimental milling conditions: milling method, energy input, powder mass, number and mass of the milling balls, addition of PCA, atmosphere, etc. Many factors, hence, affect the kinetics of milling and can determine effects such as the time needed to successfully complete a milling process [9–11], provoke reactions [9], modify the reaction times [9, 10], change the degree of material deformation [9, 10], set limits to the powder size [12] or to get amorphisation of intermetallics [13]. Specifically, it might be expected that an increase in density of the milling balls would favour the reactivity of the powder charge, since collisions between the milling bodies produce a good mixing between the reactant particles and create lattice defects that enhance chemical activity. In addition, the impacts also create hot spots where a reaction can begin.

On the other hand, MA Al powder surfaces are covered by oxide/hydroxide layers. The presence of a surface oxide film is common to Al-base powders. The oxide thickness on Al atomised powders, for instance, is around 5 nm [14]. The oxide layer of any Al-base powder is a barrier to sintering, since it inhibits material transport and the formation of necks between metal particles. Hence, the oxide film must be disrupted to allow sintering. Some rupture of the Al oxide film occurs during pressing, and local metal contacts are created. The extent of these contacts is very much depending on the plasticity of metal particles. In this respect, MA Al powder, which is very hard, lacks plasticity. Both characteristics (surface oxide films and hardness) make MA Al powders very difficult to sinter. Therefore, MA Al powder is typically consolidated by a complicated process, which includes a stage of hot extrusion [15]. At the University of Seville, an alternative

*Author to whom all correspondence should be addressed.

TABLE I Milling conditions

Vessel volume	1400 cm^3
Charge ratio:balls/powder	50:1
Mass of powder	72 g
PCA	3% EBS
Rotor speed	500 rpm
Cooling	H_2O flow (28°C)
Milling time	10 h

press-and-sinter consolidation method has been used [16, 17]. The new method could be of interest for the production of large batches of small parts.

In the present work, the influence of the milling-balls density on the characteristics of MA Al powders, and the materials consolidated from them, is investigated. Milling was carried out in vacuum, using either tungsten carbide or steel balls. MA Al powders were consolidated by a press-and-sinter technique. Final materials were studied concerning mechanical properties and fracture behaviour.

2. Experimental procedure

A commercial atomised Al powder (Eckart), 99.7 wt% Al, with 0.20 wt% Fe as main impurity, mean size 44 μm, was used as starting material. The as-received Al powder was mechanically alloyed by vacuum milling in a Szegvari attritor for 10 h. EBS (ethylene-bis-stearamide) powder, from Clariant, was employed both as PCA, during milling (3 wt% EBS), and as die-wall lubricant during cold pressing. Two types of milling balls, of different density, were used, either 4.65 mm AISI 52100 steel balls (specific gravity 7.8 $g \cdot cm^{-3}$) or tungsten carbide (WC-Co) balls (specific gravity 14.3 $g \cdot cm^{-3}$). The latter ones are not actually balls, but two semispheres united by a cylindrical rod of 4.85 mm diameter, the total length being 4.65 mm. Milling conditions are summarized in Table I.

The milled powders were consolidated by cold uniaxial pressing (850 MPa) and vacuum (5 Pa) sintering at 650°C for 1 h, followed by furnace cooling. Such a high sintering temperature, near the melting point of aluminium, was used to force diffusion processes.

Cylindrical and "dog-bone" shaped compacts (mass 4 g) were prepared. Cylindrical compacts (12 mm diameter) were used for density and hardness determinations, while dog-bone specimens (32 × 4 × 4 mm), for tensile tests [16]. The tensile specimens are basically in agreement with the corresponding MPIF [18] (Metal Powder Industries Federation) and ASTM [19] (American Society for Testing and Materials) standards. Porosity was determined by image analysis. Structural and fractographic studies by optical microscopy, quantitative metallography, X-rays diffraction (XRD), energy dispersive X-rays (EDX) spectrometry, scanning electron microscopy (SEM) and transmission electron microscopy (TEM) were also carried out.

3. Results and discussion

Milled powders were designated MA Al/S and MA Al/W, respectively, depending on the nature of the milling balls (steel or WC-Co) used. Milling brought about changes in the size and shape of the Al particles. The average particle size decreases from 44 to 17 μm, and the particles are rounder than before milling. Concerning size and shape, no difference between the powders milled with steel or hard-metal balls was found.

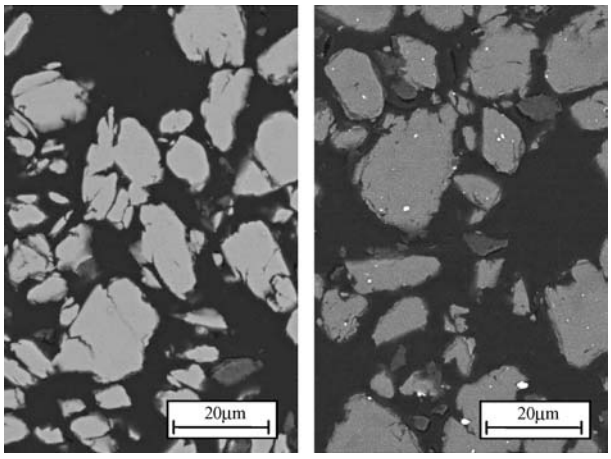

Figure 1 BSE-SEM microstructures of the MA Al/S (left) and MA Al/W (right) powders.

The MA Al/S powder shows a homogeneous microstructure where second phases are not observed by optical microscopy or SEM (Fig. 1, left). The microstructure of the MA Al/W powder is relatively similar. However, the milled particles have incorporated fragments of an inclusion (white spots), as can be seen in Fig. 1, right. This inclusion, as determined by EDX, has the same chemical composition as the hard-metal balls, i.e., 5.5 wt% Co, 0.5 wt% Ni, balance tungsten carbide.

So, the hard-metal balls have contaminated the milled Al powder. The high density of these balls increases the impact energy. This, combined with the inherent brittleness of the tungsten carbide, results in the detachment of small bits, around 3 μm of size, from the balls. The small fragments are continuously fractured by the subsequent impacts, and incorporated into the aluminium mass. After milling, the SEM microstructure shown in Fig. 1 (right) can be observed.

The microstructure of MA Al/S consolidated samples possess an Al-Fe intermetallics, $Al_{13}Fe_4$, embedded in the Al matrix (Fig. 2, left). This intermetallics is formed from the iron contained in the as-received Al powder as an impurity (0.2 wt% Fe). The solubility of iron in Al is very low, about 0.04 wt% Fe at the eutectic temperature [20]. For a 0.2 wt% Fe content, the equilibrium phases are Al solid solution and $Al_{13}Fe_4$. The Al-Fe intermetallics is large in size and needle-shaped, the mean needle area being 11.2 μm^2.

It is well known the influence of the intermetallics shape in the fracture behaviour of Al-base materials. Specifically, for Al-Fe intermetallics with acicular morphology, it has been observed that tensile fracture is favoured by the presence of these second phases. The fracture of these intermetallic compounds is of the brittle type. Moreover, fracture of tensile specimens takes place through regions where the intermetallic needles are the largest in size [21]. Therefore, the shape and

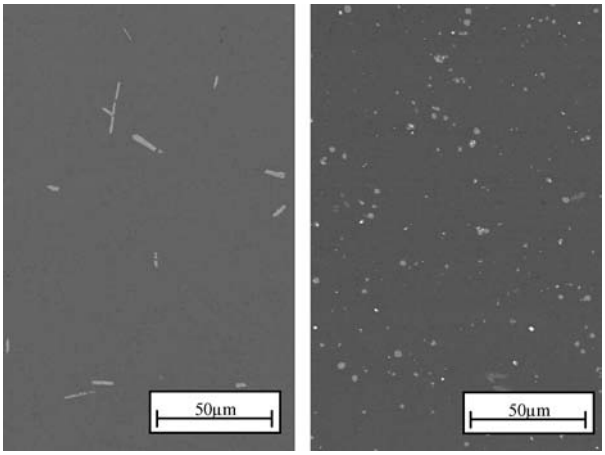

Figure 2 BSE-SEM microstructures of the MA Al/S (left) and MA Al/W (right) consolidated specimens.

dimensional control of intermetallics phases is important to improve tensile properties.

To avoid the appearance of needle-shaped Al-Fe intermetallics in aluminium casting alloys, two ways are usually followed, either to restrain the Fe content [22] or to add certain elements, like Mn and/or Cr [22, 23], that change the acicular morphology of the intermetallics. The first approach is difficult to fulfill in an industrial process; hence, the second method is customarily employed.

On the other hand, the microstructure of consolidated specimens of MA Al/W is very different of the microstructure above described, as can be assessed by comparing Fig. 2 (right) with Fig. 2 (left). The intermetallics of MA Al/W specimens are small and round-shaped. The area occupied by one of these intermetallics is 1.0 μm^2 against 11.2 μm^2 for the Al-Fe compounds in the MA Al/S material.

A careful examination by SEM, combined with EDX microanalysis, distinguishes, in addition to the matrix, two types of second phases in the MA Al/W material (Fig. 3). Both constituents are round-shaped. The one is an Al-Fe-Co-Ni intermetallics, the other one is actually a mixed phase constituted by an Al-Fe intermetallics that surrounds a nucleus of WC. An interesting result, not reported previously in the technical literature, is

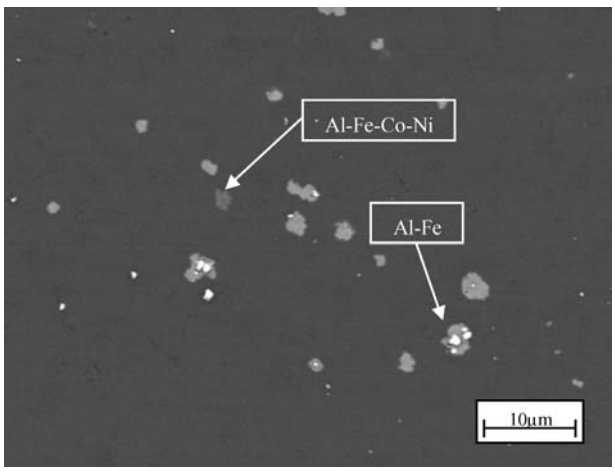

Figure 3 BSE-SEM microstructure of MA Al/W consolidated specimen, showing the intermetallics. White spots are WC particles.

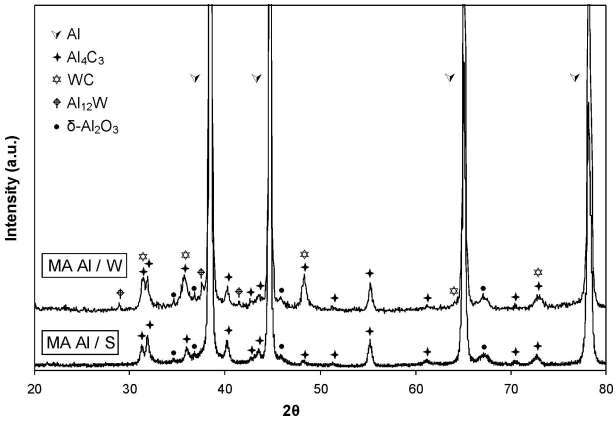

Figure 4 XRD patterns of powders, vacuum heat-treated at 650°C for 1 h.

that WC is capable to round the needle-shaped Al-Fe intermetallics in Al alloys. The WC appears as white spots (mean area ca. 0.3 μm^2) in Fig. 3.

Referring to the Al-Fe-Co-Ni intermetallics, Co is an element, like Mn and Cr, able to transform the acicular Al-Fe intermetallics in Al casting alloys into spheroidal ones [23]. The Co in the Al-Fe-Co-Ni intermetallics comes from the hard-metal ball fragments detached during attrition milling of the Al powder and the subsequent diffusion and reaction during sintering. The result is the formation of irregular spheroids of the Al-Fe-Co-Ni intermetallic compound. The presence of Ni is justified because this metal normally accompany, as an impurity, to Co, from which it is very difficult to separate.

XRD patterns, of MA Al/S and MA Al/W powders, after heating at 650°C for 1 h, are displayed in Fig. 4. XRD patterns were obtained using a Cu Kα radiation ($\lambda = 0.154056$ nm). Both heat-treated powders show peaks of Al, Al_4C_3 and δ-Al_2O_3. The Al_4C_3 is formed by reaction of aluminium with the EBS used as PCA. The aluminium carbide appears as small rods in consolidated samples observed by TEM (Fig. 5), and the mean size of aluminium grains in these samples, measured by TEM, is 550 nm. They can, thus, be considered ultra-fine-grained materials

Nevertheless, the comparison of the XRD patterns from both heat-treated powders (Fig. 4) indicates that the Al_4C_3 peaks of the MA Al/W powder, situated at 2θ angles of 31.1°, 35.5° and 48.1°, have relative intensities higher than in the same position of the MA Al/S powder. This could be explained by the presence of WC in the MA Al/W powder, since WC and Al_4C_3 have coincident reflections at these angles. On the other hand, the reduction of WC by Al, according to the reaction $3WC + 4Al \leftrightarrow Al_4C_3 + 3W$ is possible under a thermodynamic point of view, as can be easily checked by looking at the corresponding Ellingham diagram [24]. Reduction of the WC by aluminium could have taken place as a mechanochemical reaction during milling. One of the most salient features of mechanical alloying is precisely that it can trigger, at near-ambient levels, reactions that usually require a high temperature [4]. The detection of weak peaks of $Al_{12}W$ in the MA Al/W powder (Fig. 4) points out that, at least, a partial decomposition of WC has taken place.

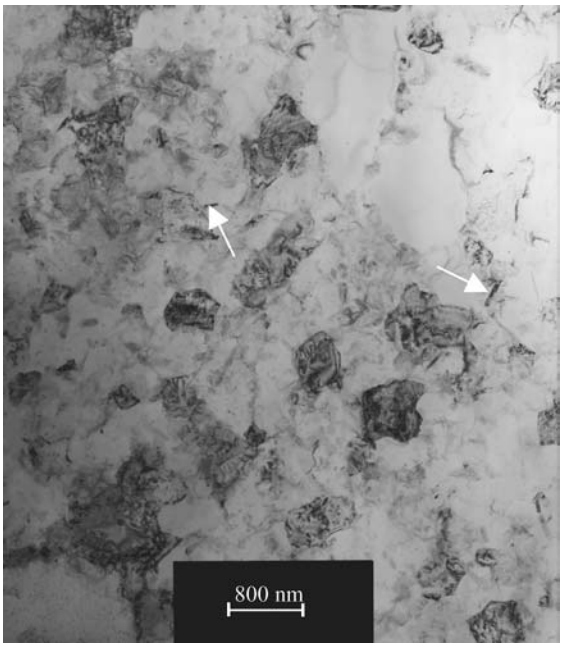

Figure 5 TEM bright field image of MA Al/S specimen. Arrows point to Al_4C_3 particles. Dark-grey polygonal patches are Al grains.

All consolidated specimens reach a high degree of densification, since the residual porosity is 3% or less. The degree of densification is the same in the MA Al/S and MA Al /W materials. The values of Brinell hardness (HB), ultimate tensile strength (UTS) and elongation (E) of the consolidated materials are shown in Table II.

Both materials, MA Al/S and MA Al/W, have about the same hardness (ca. 96 HB) and ultimate strength (ca. 300 MPa). This value of strength is worthy of notice taking into account that they are P/M (powder metallurgy) Al materials, consolidated by a press-and-sinter method, and where the typical strengthening methods of solid solution and aging have not been used. For comparison, the tensile strength of P/M Al specimens, prepared from unmilled elemental Al powder, consolidated under similar conditions, is 67 MPa, i.e., the UTS of the materials displayed in Table II is about 4.5 times higher than that of P/M elemental Al. The significant increase in tensile strength achieved for MA Al consolidated specimens is due to the dispersion-strengthening effect caused by the presence of abundant submicroscopic dispersoids of Al_4C_3 and Al_2O_3 [8]. In addition, MA Al consolidated specimens have an ultra-fine grain size of about 550 nm, as previously indicated. The fine grain size can be explained because the submicroscopic dispersoids restrain grain growth during sintering.

The remarkable microstructural difference between the two MA Al materials, above described, has a clear effect on ductility (Table II). The elongation of MA Al/S is 1.1% against 4.0% for MA Al/W. The elongation of the material with spheroidal intermetallics (Fig. 2, right) is 4 times higher than that of the material with acicular intermetallics (Fig. 2, left). The intermetallics in the MA Al/W material are not only rounder, but also smaller (1.0 μm^2 versus 11.2 μm^2) than in the MA Al/S one.

TABLE II Mechanical properties of consolidated materials

Material	HB	UTS (MPa)	E (%)
MA Al/S	96	302	1.1 ± 0.2
MA Al/W	97	290	4.0 ± 0.2

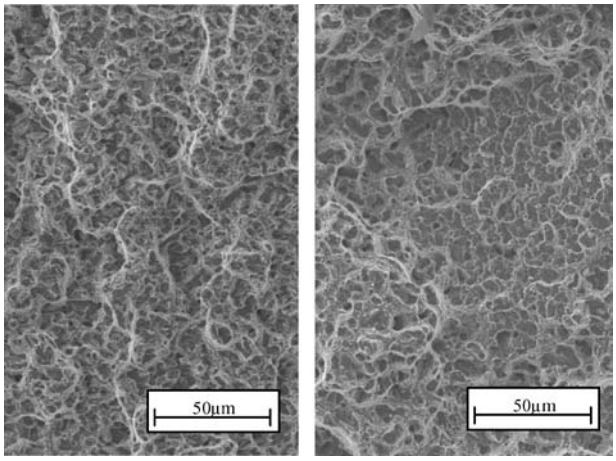

Figure 6 SE-SEM fractographs of MA Al/S (left) and MA Al/W (right) specimens broken by tensile stress. Numerous dimples can be observed.

The microfractographic study of the broken tensile specimens shows that the fracture is of the ductile type in both materials (Fig. 6). Numerous dimples, similar in size and quantity for both materials, can be seen.

Concerning the precise mechanism of fracture, SEM observations can be interpreted as fracture beginning by cleavage of the intermetallics, either needles or spheroids. Cleavage occurs in the intermetallics, not at the intermetallics-matrix interface. Then, the different cavities or microvoids, so originated, unite by ductile fracture of the metallic regions connecting them. In this way, a crack is formed. Finally, the main crack propagates reaching the external surfaces of the specimen, which breaks. The residual porosity of the specimens should behave in a similar manner to the generated cavities.

On the other hand, the fracture profiles of the two materials, observed by optical microscopy, have a distinct aspect, indicating a different fracture behaviour. In the

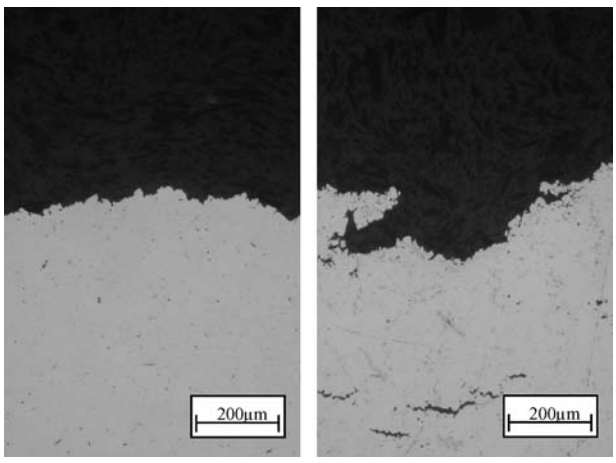

Figure 7 Fracture profiles of tensile specimens as observed by optical microscopy. MA Al/S profile (left) consists of a unique irregular surface, however MA Al/W profile (right) consists of a tortuous surface with several incipient cracks nearby.

MA Al/S specimens (Fig. 7, left), the fracture profile is a unique irregular surface, with no adjacent cavities or incipient cracks. However, as can be observed in Fig. 7, right, the profile of the MA Al/W specimens show a high degree of plastic deformation. Fracture has occurred, as it is typical in ductile materials, by coalescence of a group of cavities, and zigzag growth of the most favourable crack, until reaching the sample surfaces. Numerous tearing, in the vicinity of the fracture surface, can also be observed (Fig. 7, right). It can be concluded that crack growth is easier in MA Al/S (Fig. 7, left) than in MA Al/W (Fig. 7, right).

4. Conclusions

MA Al specimens, consolidated by cold pressing and sintering, are high-density P/M products, since final porosity is 3% or less. They also possess a high tensile strength, around 300 MPa. This value is 4.5 times higher than the UTS of P/M elemental aluminium.

The ductility of the MA Al specimens depends on the nature of balls (hardened steel or hard-metal balls) used in the attrition milling process.

The microstructure of consolidated MA Al/S specimens, prepared from powder milled with steel balls, presents large needles of an Al-Fe intermetallics. The presence of this second phase has a negative effect on ductility, which is limited to an elongation of about 1%.

The microstructure of consolidated specimens of MA Al/W, prepared from powder milled with hard-metal balls, presents very small spheroidal Al-Fe-base intermetallics. The rounding of these intermetallics is ascribed to the presence of Co and WC coming from contamination during milling. The change in size and shape of the intermetallics favorably affects the elongation, which reaches 4.0%.

Acknowledgements

The financial support of the MCYT/FEDER, Madrid, through the research project DPI 2002-00726 is gratefully acknowledged.

References

1. C. C. KOCH, *Ann. Rev. Mater. Sci.* **19** (1989) 121.
2. L. LÜ and M. O. LAI, in "Mechanical Alloying" (Kluwer Academic Publishers, Boston, MA, 1998).
3. H. BAKKER, C. F. ZHOU and H. YANG, *Prog. Mater. Sci.* **39** (1995) 159.
4. C. SURYANARAYANA, *ibid.* **46** (2001) 1.
5. KYOUNG IL MOON and KYUNG SUB LEE, *J. Alloys Comp.* **333** (1/2) (2002) 249.
6. J. A. RODRIGUEZ, J. M. GALLARDO and E. J. HERRERA, *J. Mat. Sci.* **32** (1997) 3535.
7. J. L. HERRERO, J. A. RODRÍGUEZ and E. J. HERRERA, in Proceedings of the 1998 Powder Metallurgy World Congress, Granada, October, 1998 (EPMA, Bellstone, Shrewsbury, UK, 1998), Vol. 1, p. 384.
8. R. F. SINGER, W. C. OLIVER and W. D. NIX, *Metall. Trans. A* **11** (1980) 1895.
9. G. B. SCHAFFER and P. G. MCCORMICK, *ibid.* **23** (1992) 1285.
10. G. B. SCHAFFER and J. S. FORRESTER, *J. Mat. Sci.* **32** (1997) 3157.
11. H. ZHANG and X. LIU, *Int. J. Refr. Met. Hard Mat.* **19** (2001) 203.
12. H. J. RYU, S. H. HONG and W. H. BAEK, *J. Mat. Process. Techn.* **63** (1997) 292.
13. Y. H. PARK, H. HASHIMOTO and R. WATANABE, *Mat. Sci. Forum* **88–90** (1992) 59.
14. M. NARANJO, J. A. RODRIGUEZ and E. J. HERRERA, *Scr. Mater.* **49** (2003) 65.
15. W. T. NACHTRAB and P. R. ROBERST, in "Advances in Powder Metallurgy and Particulate Materials" (MPIF, Princeton, NJ, USA 1992), Vol. 4, p. 321.
16. J. A. RODRÍGUEZ, J. M. GALLARDO and E. J. HERRERA, *Mater. Trans. JIM* **36** (1995) 312.
17. J. J. FUENTES, J. A. RODRÍGUEZ and E. J. HERRERA, *Mater. Sci. Forum* **426–432** (2003) 4331.
18. "Tension Test Specimens for Pressed and Sintered Metal Powders," MPIF Standard 10, Metal Powder Industries Federation (Princeton, NJ, USA, 1963).
19. "Mechanical Testing of Steel Products," ASTM Standard Method A 370, American Society for Testing and Materials (Philadelphia, Pa, USA, 1997).
20. F. MONDOLFO, in "Aluminium Alloys: Structure and Properties" (Butterworths, London, UK, 1976) p. 282.
21. J. A. RODRÍGUEZ, J. CINTAS, J. M. GALLARDO and E. J. HERRERA, *Anales de Mecánica de la Fractura* **16** (1999) 407.
22. H. KOCH, U. HIELSCHER, H. STERNAU and A. FRANKE, in Proceedings of the TMS annual meeting, Las Vegas, February, 1995 (TMS, Warrendale, Pennsylvania, USA, 1995) p. 1011.
23. "Aluminium: Properties and Physical Metallurgy," edited by J. E. Hatch (ASM, Metals Park, Ohio, USA, 1984) p. 64, 226, 234, 348.
24. T. ROSENQVIST, in "Principles of Extractive Metallurgy" (McGraw-Hill, New York, USA, 1974) p. 527.

Received 14 October 2004
and accepted 28 February 2005